Computers and Electronics in Agriculture 204 (2023) 107498

Contents lists available at ScienceDirect

Computers and Electronics in Agriculture

journal homepage: www.elsevier.com/locate/compag

CanopyCAM – an edge-computing sensing unit for continuous measurement of canopy cover percentage of dry edible beans

Wei-zhen Liang [a,b], Joseph Oboamah [b,c], Xin Qiao [a,b,*], Yufeng Ge [a], Bob Harveson [b,d], Daran R. Rudnick [a,f], Jun Wang [e], Haishun Yang [g], Angie Gradiz [a,b]

[a] Department of Biological Systems Engineering, University of Nebraska-Lincoln, Lincoln, NE, USA
[b] Panhandle Research and Extension Center, University of Nebraska-Lincoln, Scottsbluff, NE, USA
[c] Department of Computer Science and Engineering, University of Nebraska-Lincoln, Lincoln, NE, USA
[d] Department of Plant Pathology, University of Nebraska-Lincoln, Lincoln, NE, USA
[e] Department of Chemical and Environmental Engineering, University of Iowa, Iowa City, IA, USA
[f] West Central Research and Extension Center, University of Nebraska-Lincoln, North Platte, NE, USA
[g] Department of Agronomy and Horticulture, University of Nebraska-Lincoln, Lincoln, NE, USA

ARTICLE INFO

Keywords:
Canopy Cover (CC)
Leaf area index (LAI)
Image processing
Edge computing
Internet of Things (IoT)

ABSTRACT

Canopy cover (CC) is an important indicator for crop development. Currently, CC can be estimated indirectly by measuring leaf area index (LAI) using commercially available hand-held meters. However, it does not capture the dynamics of CC. Continuous CC monitoring is essential for dry edible beans production since it can affect crop water use, weed, and disease control. It also helps growers to closely monitor "yellowness", or senescence of dry beans to decide proper irrigation cutoff timing to allow the crop to dry down for harvest. Therefore, the goal of this study was to develop a device – CanopyCAM, containing software and hardware that can monitor dry bean CC continuously. CanopyCAM utilized an in-house developed image-based algorithm, edge-computing, and Internet of Things (IoT) telemetry to process and transmit CC in real-time. In the 2021 growing season, six CanopyCAMs were developed with three installed in fully irrigated dry edible beans research plots and three installed at commercial farm fields, respectively. CC measurements were recorded at 15 min interval from 7:00 am to 7:00 pm in each day. Initially, the overall trend of CC development increased over time but fluctuations in daily readings were noticed due to changing lighting conditions which caused some overexposed images. A simple filtering algorithm was developed to remove the "noisy images". CanopyCAM measured CC ($CC_{CanopyCAM}$) were compared with CC obtained from a LI-COR Plant Canopy Analyzer (CC_{LAI}). The average error between $CC_{CanopyCAM}$ and CC_{LAI} was 2.3 %, and RMSE and R^2 were 2.95 % and 0.99, respectively. In addition, maximum CC (CC_{max}) and duration of the maximum CC (t_{max_canopy}) were identified at each installation location using the generalized reduced gradient (CRG) algorithm with nonlinear optimization. An improvement of correlation was found between dry bean yield and combination of CC_{max} and t_{max_canopy} (R^2 = 0.77, Adjusted R^2 = 0.62) as compared to yield versus CC_{max} (R^2 = 0.58) or yield versus t_{max_canopy} (R^2 = 0.45) only. This edge-computing, IoT enabled CanopyCAM, provided accurate and continuous CC readings for dry edible beans which could be used by growers and researchers for different purposes.

1. Introduction

Dry edible beans (DEBs) are important food crops in the United States (U.S.) which provide excellent sources of protein. Total U.S. DEBs production area is approximately 809,000 ha, and the leading production states are North Dakota, Nebraska, Colorado, California, and Idaho. Nebraska DEBs production averages from 57,000 to 81,000 ha annually, producing approximately 1 billion servings (NDSU, 2020). The production is concentrated in western Nebraska, where the climate is semi-arid and the warm days and cool nights provide excellent growing conditions (NDBC, 2019). Dry edible beans require 85 to 110 days to reach maturity and the maximum production potential is reached when dry bean pods are mature, filled with seed, and 80 % of foliage yellowing (NDBC, 2019).

* Corresponding author at: Department of Biological Systems Engineering, University of Nebraska-Lincoln, Lincoln, NE, USA.
E-mail address: xin.qiao@unl.edu (X. Qiao).

https://doi.org/10.1016/j.compag.2022.107498
Received 28 April 2022; Received in revised form 24 October 2022; Accepted 12 November 2022
Available online 29 November 2022
0168-1699/

Canopy cover (CC) is the layer formed by the branches and crowns of plants. During the vegetative and reproductive stages, CC is an important parameter for measuring the development and health of DEBs, and it directly relates to crop growth stage, crop height, architecture of the leaves and density of the plants (Dai et al., 2009). Canopy cover is also important for the interception and use of solar energy and for increasing canopy photosynthetic productivity (Ma et al., 2001). It also affects crop water use, yield, disease (Westgate et al., 1997) and weed development (Ma et al., 2001). The advantages of rapid canopy development in crops include greater biomass accumulation, greater yield potential, and early season weed suppression (Westgate et al., 1997) and reduction of evaporative water loss from soil.

Canopy cover is also considered a core parameter for crop models (Qiao et al., 2016). Various crop models use CC to calculate 'light use efficiency' of the crop and simulate the energy balance equations, and to enable understanding of the physical processes that occur between plants and the environment (Norman et al., 1995; Drewry et al., 2010; Colaizzi et al., 2012; Liang et al., 2021). Therefore, continuous monitoring of CC is necessary for not only providing observation of crop development but also for irrigation management, weed control, fungicide application, and crop modeling, etc.

Many prior and current studies have used commercial plant canopy analyzers such as the LAI-2000 (LI-COR Biosciences, Lincoln, NE, U.S.) to obtain leaf area index (LAI) (Norman et al. 1995; O'Neal et al., 2002; Malone et al., 2002; Colaizzi et al. 2010, 2012; Hoffman et al. 2016; Yang et al. 2018). CC can be calculated with LAI and zenith angle (Eqn. (1)).

$$CC_{LAI} = 1 - exp\left(\frac{-0.5LAI}{\cos(\theta)}\right) \tag{1}$$

where CC_{LAI} is the fraction (dimensionless, between 0 and 1) of CC appearing in the field of view, θ is the zenith angle of LAI meter, and LAI is leaf area index. To obtain CC, many studies (Colaizzi et al. 2010; Yang et al. 2018; Liang et al. 2021) have conducted manual LAI measurement once every other week or even once a month. Despite infrequent measurements by LAI, moreover, it is difficult to obtain LAI at early crop development stages since canopy can be too small for the proper use of LAI meter. In addition, such manual measurement of LAI is technically complex and labor intensive, and it is impossible to continuously measure CC in the field to account for the variations and dynamics of CC along the crop growth cycle.

Image processing has been used as an effective tool for analyses in various crops and applications. In recent years, several studies have used image processing to assess features of crop canopies for different purposes, such as determining fertility requirements, disease detection, smart spraying, and yield estimation (Diago et al., 2012; Hitimana and Gwun, 2014; Masood et al., 2016). Canopeo, an image processing tool, was developed using Matlab (The MathWorks Inc., Massachusetts, U.S.) and is based on color ratios of red to green (R/G), and blue to green (B/G), and an excess green index (2G-R-B) to determine CC (Patrignani and Ochsner, 2015). This online tool uses color classification techniques in the RGB color spectrum to distinguish canopy from background (e.g. soil) in images. However, image overexposure and soil under shadow were not considered in Canopeo, resulting in overestimation of CC when crops reach full CC (Buchi et al., 2018). To estimate the CC more accurately from images, supervised classification has been used in research studies (Chena et al., 2010; Diago et al., 2012; Liang et al., 2018; Liang et al., 2021). Several statistical measurements of similarity between groups, in terms of multiple characteristics, have been proposed, such as Kolmogorov's variation distance, Bhattacharyya distance, and Mahalanobis distance (Devroye et al., 1996). Mahalanobis distance (Md) classification is widely used for pattern recognition and data analyses when groups have different means but similar standard deviations (Devroye et al., 1996) and is most suitable in image processing for precision agriculture (Chena et al., 2010; Diago et al., 2012; Liang et al., 2018; Liang et al., 2021). Chena et al. (2010) extracted 28 color features from corn imagery using Md for identifying five Chinese corn varieties at a success rate of 90 %. Diago et al. (2012) extracted 40 color features in 7 color groups and used Md to determine each pixel from image belongs to which color group to characterize grapevines, leaves, and background. The results showed a performance of 92 % effectiveness for leaves and 98 % effectiveness for grapes. Liang et al. (2018) extracted 180 colors in 8 groups and showed a performance of 96 % for detection of soybean leaves using Md classification. The Md supervised classification was able to separate soybean leaf color from background and determine the soybean leaf pixel numbers to determine soybean defoliation caused by insect damages.

Current image processing techniques require images to be transmitted or downloaded for either server- or local processing. However, CC images can range ~ 1–4 Mb in size and it can be infeasible to transmit such images frequently due to high bandwidth requirement and costly telemetry fees. An alternative solution is to leverage edge-computing to reduce data package size and utilize low-cost Internet of Things (IoT) telemetry for low-cost and near real-time data transmission. Due to data transferring with limited network performance, the centralized cloud-computing structure becomes inefficient for processing and analyzing huge amounts of data and images collected from IoT devices. Edge computing can reduce the loads of computing tasks of the centralized cloud by conducting computation at edge IoT devices. At each edge-computing IoT device, images can be processed and only edge-processed data are transmitted to cloud server, and therefore greatly reduces data package size (Chen et al., 2018).

Long range wide area network, or LoRaWAN, is one of the data transmission protocols that has been rapidly developing for many IoT applications. With one LoRaWAN gateway, it has the capability of connecting to a large number of battery-powered sensors at low energy consumption with transmission range up to 15 km in suburban areas (LoRa Alliance, 2015; Adelantado et al. 2017). The limitation of LoRaWAN is that its data transmission rate is much lower than traditional telemetry, at a maximum speed of 27 kb/s (Adelantado et al. 2017) and therefore not suitable for directly transmitting high-volume data such as CC images. However, if images are pre-processed and stored onsite, and only processed results are transmitted, the size of data package would reduce from ~ 4 Mb to 2–3 kb which will be suitable for LoRaWAN. Hence, the objective of this paper was to develop an edge-computing camera device, named CanopyCAM that can continuously monitor CC for DEBs. Detailed objectives included: 1) develop an algorithm to estimate CC from Red-Green-Blue (RGB) imagery; 2) develop a ground-based edge-computing node that can take CC images, store and process images onsite, send processed CC value through LoRaWAN network, and display at an in-house programmed website (http://phrec-irrigation.com/); 3) evaluate performance of the software on determination of CC versus LAI meter derived CC; 4) refine the CC algorithm to filter out abnormal images; and 5) identify key CC information such as max canopy cover (CC_{max}) and duration of CC_{max} (t_{max_canopy}) and evaluate its relationship with yield of DEBs.

2. Materials and methods

The sections discussed below included hardware and software of CanopyCAM, followed by description of field sites, data collection procedures, and finally data evaluation procedures.

2.1. CanopyCAM – Hardware development and processing framework

The processing framework was shown in Fig. 1, where it started from CanopyCAM designed to acquire, store, and process images at 15 min sampling intervals from 7:00 am to 7:00 pm on a daily basis. Then the device sent processed CC percentage by CanopyCAM ($CC_{CanopyCAM}$) through nearby gateways to a cloud server and then displayed the results at a customized visualization platform (https://phrec-irrigation.com).

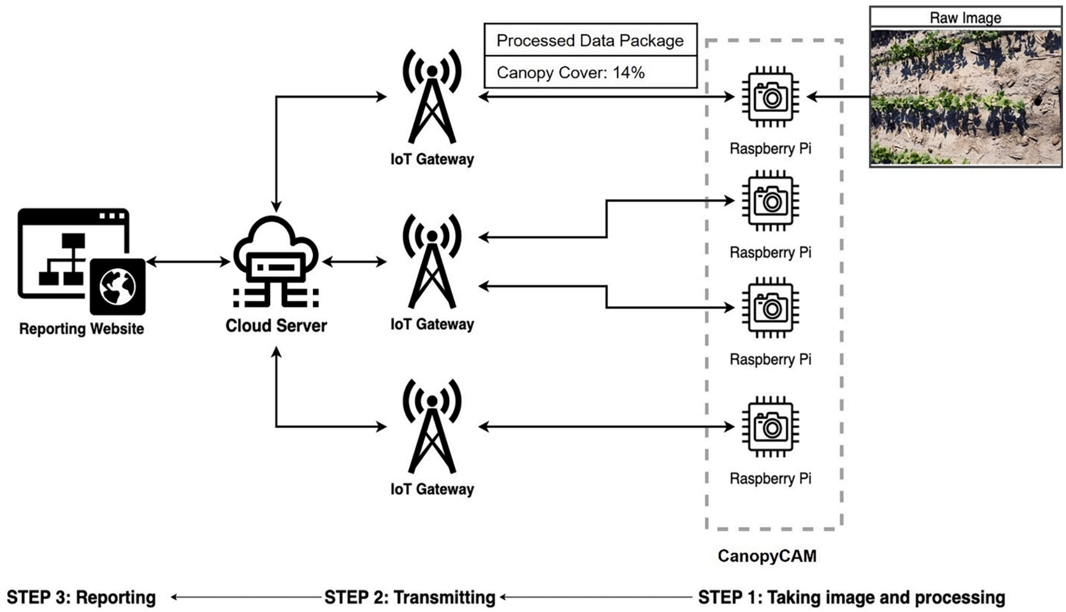

Fig. 1. Proposed processing framework to acquire and process Canopy Cover (CC) images, transmit the CC percentages through LoRaWAN gateways to a cloud server, and report the results via a cutomized website in this study.

As shown in Fig. 2c, CanopyCAM consisted of a Raspberry Pi 4 computer (Raspberry Pi foundation, U.K.), a battery, a PiJuice HAT power management board (Pi Supply, U.K.) that manages sleep and wake schedules, a solar panel, a Raspberry Pi camera module V2-8 megapixel RGB camera (2592 × 1944 pixels), Raspberry Pi LoRa node pHAT (Pi Supply, U.K.), and an external 915 MHz LoRa antenna (Laird Connectivity, Akron, OH, U.S.). It also had a DC to DC voltage regulator to convert the voltage coming in from the solar panel to 9 V (+/- 0.9 V) to the power management board. The mounting height of CanopyCAM for dry beans was determined to be 1.4 m aboveground facing north, 45 degrees off nadir-view for best image qualities (Fig. 2a, 2b). Algorithm was programmed on Raspberry Pi and images were processed onsite to calculate $CC_{CanopyCAM}$. The $CC_{CanopyCAM}$ values and other variables such as the battery status were then converted to encoded HEX value which were then transmitted to nearby LoRaWAN gateways.

2.2. Experiment site and data collection

In this study, six CanopyCAMs were deployed at three DEBs research plots at the University of Nebraska-Lincoln, Panhandle Research and Extension Center (PHREC) in Scottsbluff, NE (41°53′34.93″N, 103°41′2.04″W, elevation 1189 m), and three commercial dry bean fields in Henry and Mitchell, NE, in 2021 (Table 1). Each field or plot had one CanopyCAM installed at a representative location. The three CanopyCAMs at PHREC were installed in fully irrigated dry bean research plots. The fully irrigated plots were meant to fully satisfy crop water needs by carefully scheduling irrigation events to make sure crops were not water stressed. The commercial fields were assumed to be fully

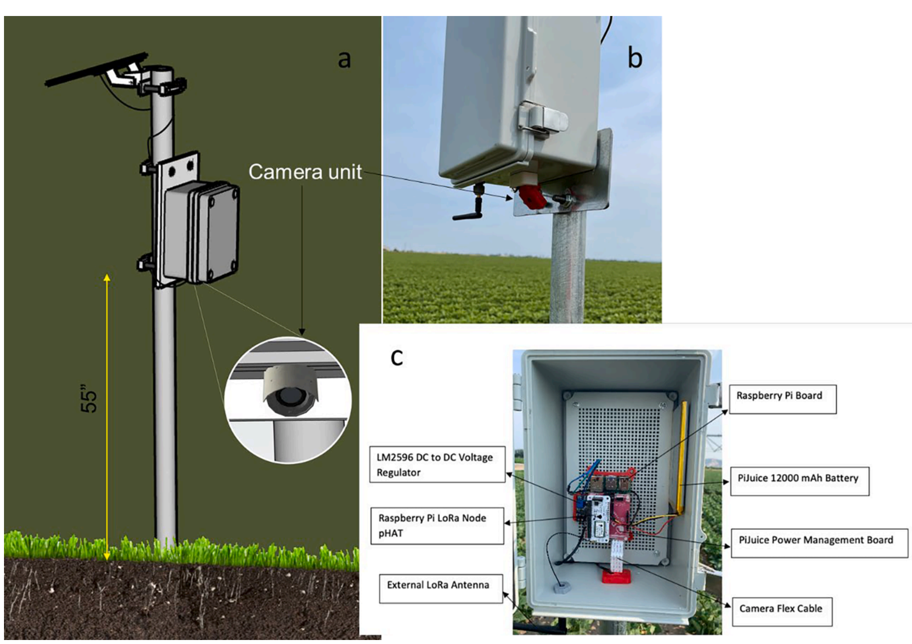

Fig. 2. a. CanopyCAM 3d illustration. b. CanopyCAM installed in field in 3d-printed casing. c. processing hub for CanopyCAM that includes raspberry pi 4 board, battery, pijuice power management board, dc to dc voltage regulator, transmissing module raspberry Pi LoRa pHAT.

Table 1
Study sites and CanopyCAM node information.

Site information ID	Loc.	Elev., m	Planting Date	Harvest Date	Start Date[1]	End Date[2]
R-1	PHREC	1189	6/1/2021	9/27/2021	6/28/2021	8/30/2021
R-2	PHREC	1189	6/1/2021	9/27/2021	7/1/2021	8/24/2021
R-3	PHREC	1189	6/1/2021	9/27/2021	7/1/2021	8/30/2021
C-1	Mitchell	1200	5/20/2021	9/10/2021	7/15/2021	8/24/2021
C-2	Henry	1231	5/27/2021	9/21/2021	7/16/2021	8/9/2021
C-3	Henry	1231	5/28/2021	9/16/2021	7/16/2021	8/25/2021

[1] Images acquisition starting date.
[2] Images acquisition end date.

irrigated according to on-site soil water sensor data (data not shown), but they were subjected to different field conditions and management practices. The climate at both research and commercial farms is semi-arid with average annual rainfall of 398 mm. Great Northern Beans were planted at 56 cm row spacing on June 1, May 27, and May 20 of 2021 at PHREC, Henry, and Mitchell, respectively. The seeding rates were 210,035 seeds ha^{-1}, 217,836 seeds ha^{-1}, and 217,448 seeds ha^{-1} at PHREC, Henry, and Mitchell, respectively. The nitrogen application rates were 85.1 kg ha^{-1}, 89.6 kg ha^{-1}, and 89.7 kg ha^{-1} at PHREC, Henry, and Mitchell, respectively. The soil textures were sandy loam, sandy loam, and sandy clay loam at PHREC, Henry, Mitchell, respectively. Beans were harvested with a commercial combine (John Deere 9500, John Deere, Moline, Illinois, U.S.) equipped with Global Positioning System (GPS) enabled yield monitor (Ag Leader Insight yield monitor, Ag Leader Technology, Inc., Ames, Iowa, U.S.) at research plots. Yield at commercial farms were obtained from weigh scale at grain elevators. Dry edible beans were harvested on 9/27/2021 at three research plots (R-1, R-2, and R-3), 9/10/2021 at commercial field 1 (C-1), 9/16/2021 at commercial field 3 (C-3), and 9/21/2021 at commercial field 2 (C-2) (Table 1). In addition to CC images, leaf area index (LAI) was manually taken twice a week at the same location of the three CanopyCAM installed at research plots (R-1, R-2, and R-3) using LAI-2000 (LI-COR Inc., Lincoln, U.S.). LAI values were converted to CC, termed as CC_{LAI} using Eqn. (1), and were used as reference CC. Simultaneously, a commercial RGB camera (Sony Cyber-shot DSC-RX100, Sony Corporation, Tokyo, Japan) was used to take images at the same height as CanopyCAM with the same shooting angle. Manual images and LAI were collected at the same time at each plot around solar noon (11:00 AM – 2:00 PM) to guarantee data and image quality. Each image taken by the handheld camera was compared with nearest timestamp image taken by CanopyCAM. The manual images also served as reference images which can be quality controlled.

2.3. CanopyCAM – Software development

2.3.1. Determination of canopy cover percentage – Crop canopy image analyzer (CCIA)

As mentioned earlier, CanopyCAM took images at every 15 min from 7:00 am to 7:00 pm on a daily basis during July and August in 2021 growing season. Thirty representative canopy images from research plots (R-1, R-2, and R-3) during different growth stages were randomly selected to classify color groups and train an in-house designed software crop canopy image analyzer (CCIA) for estimating CC_{Canopy_CAM}. CCIA utilized a supervised classifier based on Mahalanobis distance (Md) method to estimate CC, which was used to determine soybean leaf area (Liang et al. 2018) and DEBs leaf area (Liang et al. 2021). The Md (Eqn. (2)) measured the similarity between an unknown sample group and a known sample group.

$$Md = \sqrt{(X - Y)^T S^{-1} (X - Y)} \tag{2}$$

where X is a three-dimensional vector (R, G, B), which represented pixels from the image to be processed. Y is a three-dimensional vector ($\overline{R}$, $\overline{G}$, $\overline{B}$), which represented the average of reference pixels (reference group) for each class to be identified. The Mahalanobis color distance standardizes the influence of the distribution of each feature considering the correlation between each pair of terms. In the case of RGB color images, S is computed as (Eqn. (3)):

$$S = \begin{bmatrix} \sigma_{R_{ref}R_{ref}} & \sigma_{R_{ref}G_{ref}} & \sigma_{R_{ref}B_{ref}} \\ \sigma_{G_{ref}R_{ref}} & \sigma_{G_{ref}G_{ref}} & \sigma_{G_{ref}B_{ref}} \\ \sigma_{B_{ref}R_{ref}} & \sigma_{B_{ref}G_{ref}} & \sigma_{B_{ref}B_{ref}} \end{bmatrix} \tag{3}$$

and as an example, the elements of S are calculated as:

$$\sigma_{G_{ref}R_{ref}} = \sigma_{R_{ref}G_{ref}} = \frac{\sum_{i=1}^{n} (R_i - \overline{R})(G_i - \overline{G})}{n - 1} \tag{4}$$

where σ is covariance of R, G, B reference group colors, R_i, G_i, B_i are the values of the i^{th} match (i = 1, 2, 3, ….n), and $\overline{R}$, $\overline{G}$, $\overline{B}$ are the mean color values for R, G, B in the given image, respectively.

In this study, eight reference groups of pixels were selected to generate the classification, in which every group represented relevant characteristics of dry bean leaves and background classes, as well as installation environment of CanopyCAM. The eight groups were identified as: light green leaves, light yellow leaves, dark green leaves, greyish green leaves, shadow, light-colored soil, deep-colored soil, and silver-colored metal post on which CanopyCAM were attached. If any of these classes were not present, or a new class appeared on the image, the number and/or the group labels would be modified. Each reference group was manually selected from a set of 30 canopy images and a set of 20–30 color pixels with R, G, B, values in each reference group was chosen. The 30 canopy images were used to train CCIA so pixels could be classified into the right color group. After training CCIA, Md was computed over a set of 11,206 images from the six CanopyCAM devices installed during the 2021 growing season. CCIA was written in C++ programming language (Stroustrup, 1995) and was programed on CanopyCAM since Raspberry Pi lacks GPU and has limited computation power. After images were processed in CanopyCAM, the outputs of canopy pixels, background pixels, battery power, and $CC_{CanopyCAM}$ were transmitted to the IoT gateways and back to the cloud server. Identified CC were shown as pink color and the background was shown as original color in the output images. The $CC_{CanopyCAM}$ percentage was calculated using green area pixel number (N_G) and background pixel number (N_B) (Eqn.5).

$$CC_{CanopyCAM} = \frac{N_G}{N_G + N_B} \times 100\% \tag{5}$$

2.3.2. Post-processing: Image filtering algorithm

After evaluating the images from the six CanopyCAM units, it was noticed that the overall trend of CC development increased over time but there were large variations in daily readings. Upon inspection of the large daily variations of $CC_{CanopyCAM}$, some were caused by images that were taken in poor lighting conditions (e.g. overexposure) that interfered with the camera. Overexposure was caused when too much light hits camera's sensor and resulted extremely bright images. An example of overexposed raw and processed images from CanopyCAM were shown in Fig. 6. When images were overexposed, $CC_{canopyCAM}$ were underestimated. Therefore, a 2-step filtering processes was created to filter out the overexposed images. First, images prior to 10:00 am and after 4:00 pm were filtered out because the sunlight could enter the camera lens at more parallel angles. Subsequently, the color intensity of each pixel of the images (Y) was calculated (Eqn. (6)), and when Y was greater than 224, the pixel was determined to be an overexposed pixel. If the percentage of overexposed pixels was greater than 50 %, or if the $CC_{CanopyCAM}$ percentage was increased or reduced by more than 10% compared to the previous image (indicating too much variation), the CC image was removed.

$$Y = 0.299 \times R + 0.587 \times G + 0.114 \times B \tag{6}$$

where Y is color intensity of the pixel, R is red color value, G is green color value, B is blue color value, and the values are between 0 and 255.

2.4. Evaluation of $CC_{CanopyCAM}$, CC_{LAI}, and $CC_{Handheld\_Camera}$

To determine the accuracy of $CC_{CanopyCAM}$, root mean square error (RMSE) values for pairs of $CC_{CanopyCAM}$ versus CC_{LAI}, and $CC_{Handheld\_Camera}$ versus CC_{LAI}, daily averaged canopy cover from CanopyCAM after post processing ($CC_{ave\_CanopyCAM}$) images versus CC_{LAI} were calculated using:

$$RMSE = \sqrt{\frac{\sum_{i=1}^{n}(E-M)_i^2}{n}} \tag{7}$$

where n is number of measurements; and E and M are estimated values (from CanopyCAM/handheld camera/average daily CanopyCAM) and measured values (from LAI), respectively.

Average error for pairs of $CC_{CanopyCAM}$ versus CC_{LAI}, and $CC_{Handheld\_Camera}$ versus CC_{LAI}, daily averaged canopy cover from CanopyCAM after post processing ($CC_{ave\_CanopyCAM}$) images versus CC_{LAI} were calculated using:

$$Average\ error = \frac{\sum|E-M|}{n} \tag{8}$$

where n is number of measurements; and E and M are estimated values (from CanopyCAM/handheld camera/average daily CanopyCAM) and measured values (from LAI), respectively.

2.5. Determination of maximum canopy cover (CC_{max}) and its duration (t_{max_canopy})

In this study, we categorized the development of CC for DEBs into three stages. The first stage is mostly vegetative development when CC gradually increase to a maximum (CC_{max}). The second stage is mostly reproductive stage when CC remains nearly constant and dry beans are flowering and developing pods. The third stage is senescence when leaf starts to turn yellow, and CC starts to decrease as dry beans approach maturity. It should be noted that this categorization follows numerical value of CC rather than agronomically determined growth stage, as DEBs could be developing its canopy size while entering reproductive stage. The number of days that DEBs take to reach from planting to beginning of second stage is termed as t_1 and is normally less or equal to 56 days after planting (NDSU, 2019). The duration of CC_{max} during the second stage, termed as t_{max_canopy} would continue for 15–40 days, depending on the beans variety, field environment, and management. The end time of CC_{max} is defined as t_2, and the t_{max_canopy} is defined as t_2-t_1. It was hypothesized that the combination of CC_{max} and t_{max_canopy} would closely relate to yield of DEBs. The daily $CC_{ave\_CanopyCAM}$ was used for estimating t_1 and t_2. The generalized reduced gradient (CRG) algorithm and constraints (Eqns. (9) and (10)) in Microsoft Excel Solver (Microsoft Excel, Microsoft Corporation, 2018.) were used with nonlinear optimization to obtain the t_1 and t_2 at each CanopyCAM location.

$$\left\langle \begin{array}{c} t_1 \le 56 \\ t_1 = integer \\ t_1 \ge initial\ day \end{array} \right. \tag{9}$$

The CC_{max} is decreased after reproductive stage R_8 (82 days after planting) (NDSU, 2019). The estimated CC_{max} was averaged during t_2-t_1 interval.

$$\left\langle \begin{array}{c} t_2 \le the\ harvest\ day \\ t_2 = integer \\ t_2 \ge 82 \end{array} \right. \tag{10}$$

2.6. Statistical regression of dry edible beans yield

Empirical model for yield of DEBs from research plots and commercial fields were developed to evaluate statistical trends in the data. A simplified multiple variable regression analysis (using SAS procedure PROC REG) (SAS, 2014, Institute SAS Inc., Cary, NC) was used to generate linear regression for dry bean yield with CC_{max} and t_{max_canopy}.

3. Results and discussion

3.1. Performance of software

Using current configuration of CanopyCAM, it took 2–3 seconds to process one image (resolution 2592 × 1944). Processed data were sent through nearby LoRaWAN gateways and saved on server's database and shown at a customized reporting website. An example of CanopyCAM reported original $CC_{CanopyCAM}$ at R-1 on the website is shown in Fig. 3.

At the three research sites: R-1, R-2, and R-3, CanopyCAM collected a total of 2422, 2238, and 2394 images, respectively (Table 2). At commercial farms: C-1, C-2, and C-3, CanopyCAM collected a total of 1483, 1041, and 1628 images, respectively (Table 2). CanopyCAM collected fewer images at commercial farm fields than research plots since they were deployed later and retrieved earlier to avoid interference with growers' planting/spraying/harvesting operations. Table 2 also listed standard deviation of daily $CC_{CanopyCAM}$ readings. It was assumed that CC should remain constant during the day and standard deviation (SD) was computed for daily $CC_{CanopyCAM}$ readings (Table 2). Original $CC_{CanopyCAM}$ showed large variation during the day with SD as much as 22.1 % (Table 2, R-1 plot). An example of dry bean canopy (raw and processed images, taken on 7/7/2021 at R-1) during vegetative stage taken by CanopyCAM was shown in Fig. 4. While Fig. 5 showed an example of dry bean canopy (raw and processed images, taken on 8/27/2021 at R-1) during senescence stage when dry beans were ready to be harvested. It was observed that dark-colored soil pixels, crop residual pixels, and shadows pixels were properly classified and filtered (Fig. 5). The classifiers for eight reference groups performed well without any adjustments of contrast, brightness, or color. However, as mentioned in the material and methods section, overexposed images were also noticed (Fig. 6). Overexposure resulted underestimation of $CC_{CanopyCAM}$. For example, at R-1, CanopyCAM reported CC of 26 % on 7/22/2021 (Fig. 6), a decrease from 37 % reported on 7/7/2021 (Fig. 4). Since it was still during vegetative stage, $CC_{CanopyCAM}$ on 7/22/2021 should be larger than $CC_{CanopyCAM}$ on 7/7/2021. Post-processing algorithm (described in 2.3.2) was applied to all CanopyCAM images downloaded from the six CanopyCAMs. Post processing has effectively reduced SD of daily $CC_{CanopyCAM}$ readings to 2.2–7.5 % (Table 2).

As shown in Fig. 7a-c and Fig. 8a-c, it further demonstrated large daily variations of original $CC_{CanopyCAM}$ (black hollow circles) due to overexposure and other possible abnormal lighting conditions. The CC images were not available for C-2 after August 10th due to battery power and LoRa signal issues (Fig. 8b). The post-processing process removed most of the daily variations and provided more reasonable CC curves for CC development (Fig. 7a-c and Fig. 8a-c, red solid dots). The commercial farms also exhibited different CC trends as C-1 (Fig. 8a) appeared to

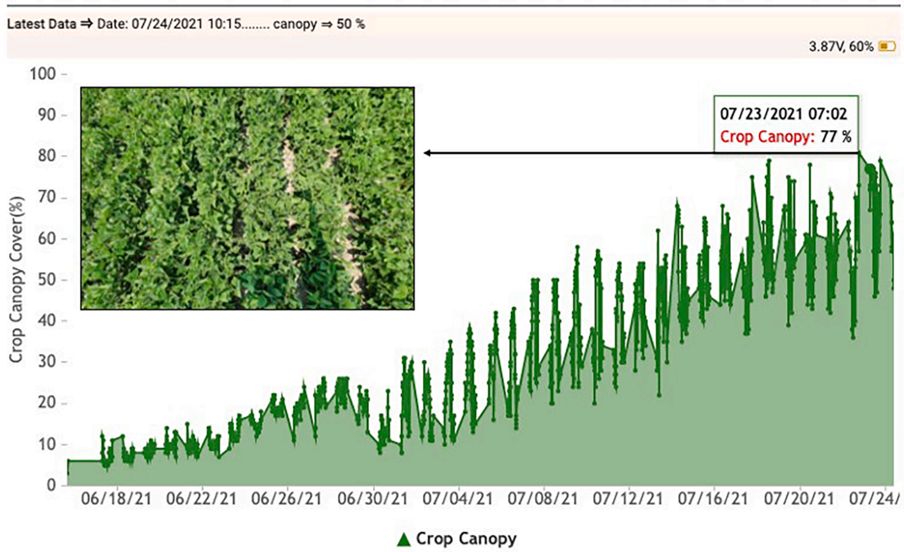

Fig. 3. Continuous canopy cover percentage of original images captured using CanopyCAM at a fully-irrigated dry edible research plot at R-1, Panhandle Research and Extension Center, University of Nebraska-Lincoln.

Table 2
Number of original and post-processed images, as well as standard deviations (SD) of daily canopy cover (CC) readings at each site.

Site	Image #[1]	SD[4]	#[2]	SD[5]	#[3]	SD[6]
R-1	2422	6.8–22.1 %	1509	5.2–14.2 %	1325	2.4–6.8 %
R-2	2238	6.2–19.8 %	802	5.8–13.1 %	688	2.3–5.9 %
R-3	2394	7.1–20.3 %	956	6.7–13.8 %	852	2.2–5.8 %
C-1	1483	5.9–18.7 %	702	4.3–12.8 %	649	2.7–5.3 %
C-2	1041	6.4–19.2 %	530	5.2–13.7 %	512	2.5–4.6 %
C-3	1628	4.7–15.3 %	469	4.2–11.5 %	463	2.8–7.5 %

[1] Number of images downloaded from CanopyCAM at each site.
[2] Number of images applied 1st step filter process which is time-based filtering. Images collected prior to 10:00 am and after 4:00 pm were filtered.
[3] Number of images applied 2nd step filer process which is lightness-based filtering.
[4] Standard deviation of daily original $CC_{CanopyCAM}$ readings.
[5] Standard deviation of daily $CC_{CanopyCAM}$ after 1st step filter process was applied.
[6] Standard deviation of daily $CC_{CanopyCAM}$ after 2nd step filter process was applied.

have larger CC than C-2 (Fig. 8b) and C-3 (Fig. 8c). This was possible due to soil texture at C-1 was sandy clay loam, which had better water holding capacity compared to C-2 and C-3 with sandy loam soil. Also, C-1, C-2, and C-3 belong to different growers and could subject to different management practices and therefore exhibited different CC patterns. Lastly, white mold disease was found at C-3 and caused lower CC at C-3 compared to C-1 and C-2.

Before evaluating performance of CanopyCAM, CC recognized from images taken using handheld camera ($CC_{Handheld\_camera}$) were evaluated against CC from LAI (CC_{LAI}). Images from handheld camera were considered to have the best image quality and were processed using the same software (CCIA) that was programmed on CanopyCAM. Good agreement between $CC_{Handheld\_camera}$ with CC_{LAI} would indicate good performance of CCIA and confirm confidence with the algorithm. A total of 41 pairs of $CC_{Handheld\_camera}$ with CC_{LAI} collected from 7/2/2021 to 8/24/2021 at R-1, R-2, and R-3 research plots were compared (n = 41). The average error between $CC_{Handheld\_camera}$ and CC_{LAI} was 2.0 %, and RMSE and R^2 were 2.64 % and 0.99, respectively (Fig. 9a). This indicated good performance of CCIA when image quality was satisfactory. To evaluate performance of canopy cover from CanopyCAM ($CC_{CanopyCAM}$) versus CC_{LAI}, $CC_{CanopyCAM}$ that was collected at the same time as LAI measurements were used. As shown in Fig. 9b, the average error between $CC_{CanopyCAM}$ and CC_{LAI} was 2.3 %, and RMSE and R^2 were 2.95 % and 0.99, respectively. This confirmed satisfactory performance of CanopyCAM. Furthermore, daily $CC_{CanopyCAM}$ after the two filtering processes were averaged at each CanopyCAM location ($CC_{ave\_CanopyCAM}$) and were compared with CC_{LAI}. As a result, error and RMSE of $CC_{ave\_CanopyCAM}$ with CC_{LAI} slightly increased to 5.7 % and 4.05 %, respectively; R^2 also slightly dropped to 0.98 (Fig. 9c). It was noticed that at

Original image Processed image ($CC_{CanopyCAM}$=42%)

Fig. 4. An example of original and processed canopy cover (CC) image collected by CanopyCAM at R-1 on July 7, 2021.

Original image Processed image ($CC_{CanopyCAM}$=12%)

Fig. 5. An example of original and processed canopy cover (CC) image collected by CanopyCAM at R-1 on August 28, 2021.

Original image Processed image ($CC_{CanopyCAM}$=26%)

Fig. 6. An example of original and processed overexposed canopy cover (CC) image collected by CanopyCAM at R-1 on July 22, 2021.

lower CC, $CC_{ave\_CanopyCAM}$ was lower than CC_{LAI}. This was possibly due to variations occurred during the senescence stage as leaves were yellowing before harvest. The color of deep yellow group could be added to CCIA and could potentially solve this issue. However, the underestimation was marginal and was not addressed in this study. Overall, $CC_{CanopyCAM}$, $CC_{Handheld\_camera}$, and $CC_{ave\_CanopyCAM}$ all provided satisfactory estimation of CC compared to CC_{LAI}.

3.2. Evaluation of CC_{max} and t_{max_canopy}

After satisfactory performance of CanopyCAM was obtained, maximum CC (CC_{max}) and duration of maximum CC (t_{max_canopy}) were estimated using CRG algorithm and constraints (Eqns. (9) and (10)). Daily $CC_{ave\_CanopyCAM}$ were used to estimate t_1, t_2, averaged CC_{max}, and t_{max_canopy}. Fig. 10 provided an example of estimating t_1 using CRG algorithm and constraints (Eqn. (9)) at R-1 field. The t_1, t_2, average CC_{max}, t_{max_canopy}, and yield of the six fields were listed in Table 3. The CC_{max} and t_{max_canopy} were not available at C-2 due to the limited number of images and CRG algorithm could not be applied. The average CC_{max} of R-1, R-2, R-3, C-1, and C-3 were 77 %, 71 %, 79 %, 82 %, and 53 %, respectively (Table 3). Fig. 11 showed the pictures of CC_{max} at six fields on 8/9/2021. As C-2 lost power on 8/10/2021, CC image taken on 8/9/2021 was extracted for visual comparison, but it was not used in the subsequent analysis. The t_{max_canopy} at R-1, R-2, R-3, C-1 and C-3 were 33, 28, 15, 19, and 15 days, respectively (Table 3). During 2021 growing season, the dry edible beans yield of R-1, R-2, R-3, C-1, C-2, and C-3 were 436, 315, 329, 403, 322, and 248 kg ha^{-1}, respectively. Many literature have supported that CC is closely related to yield of crops such as corn (García-Martínez et al., 2020) and soybean (Schmitz et al., 2021). In this study, visual inspection has shown that when CC_{max} of dry edible beans was larger, yield was higher (Fig. 11 and Table 3). Interestingly, although CC_{max} at R-1 and R-3 were similar, t_{max_canopy} at R-1 (33 d) were much longer than R-3 (15 d). As a result, yield at R-3 (329 kg ha^{-1}) was lower than R-1 (436 kg ha^{-1}). At commercial farms, CC at C-3 was the lowest. By examining CanopyCAM images, white mold disease was suspected to occur at C-3 after flowering with some dead leaves and bleached white tissues (Fig. 11 C-3). White mold, caused by the pathogen Sclerotina sclerotiorum, is one of the most important diseases affecting dry edible beans in western Nebraska (Harveson et al., 2013). The incidence and severity of white mold can be sporadic year to year with possible yield losses reaching 20 % on average (Harveson et al., 2013). Infected stems and branches affected plant parts to wilt and die, resulting in a dried bleached appearance (Fig. 11, C-3). Later, personal communication with the grower confirmed the occurence of white mold at the C-3 field.

As previously mentioned, t_{max_canopy} could be another parameter related to yield of dry edible beans. To our best knowledge, t_{max_canopy} for DEBs is not available in the literature, possibly due to the inability to monitor CC frequently or continuously either using LAI meter, drone, or satellite images. Yet, many studies have used drone or satellite images to estimate CC using normalized difference vegetation index (NDVI) and fractional green canopy cover (FGCC) to correlate CC and yield potential at certain times of crop growing stages (Garcia-Martinez et al., 2020; Reed et al., 2021; Tenreiro et al., 2021). Discrete monitoring (bi-weekly or monthly) of CC using drone or satellite images has been a popular method to determine the relationship between CC and yield, but it does not account for the duration of maximum CC. Fig. 12a and Fig. 12b showed correlation of CC_{max} with yield ($R^2 = 0.58$) and t_{max_canopy} with yield ($R^2 = 0.45$) when they were individually considered. After conducting a multiple variable regression analysis, by considering CC_{max} and t_{max_canopy} together, the correlation with yield was improved ($R^2 = 0.77$, Adjusted $R^2 = 0.62$). It should be noted that the multiple linear regression of yield among CC_{max} and t_{max_canopy} was not significant (p-value greater than 0.05) due to the small sample size (n = 5). It should

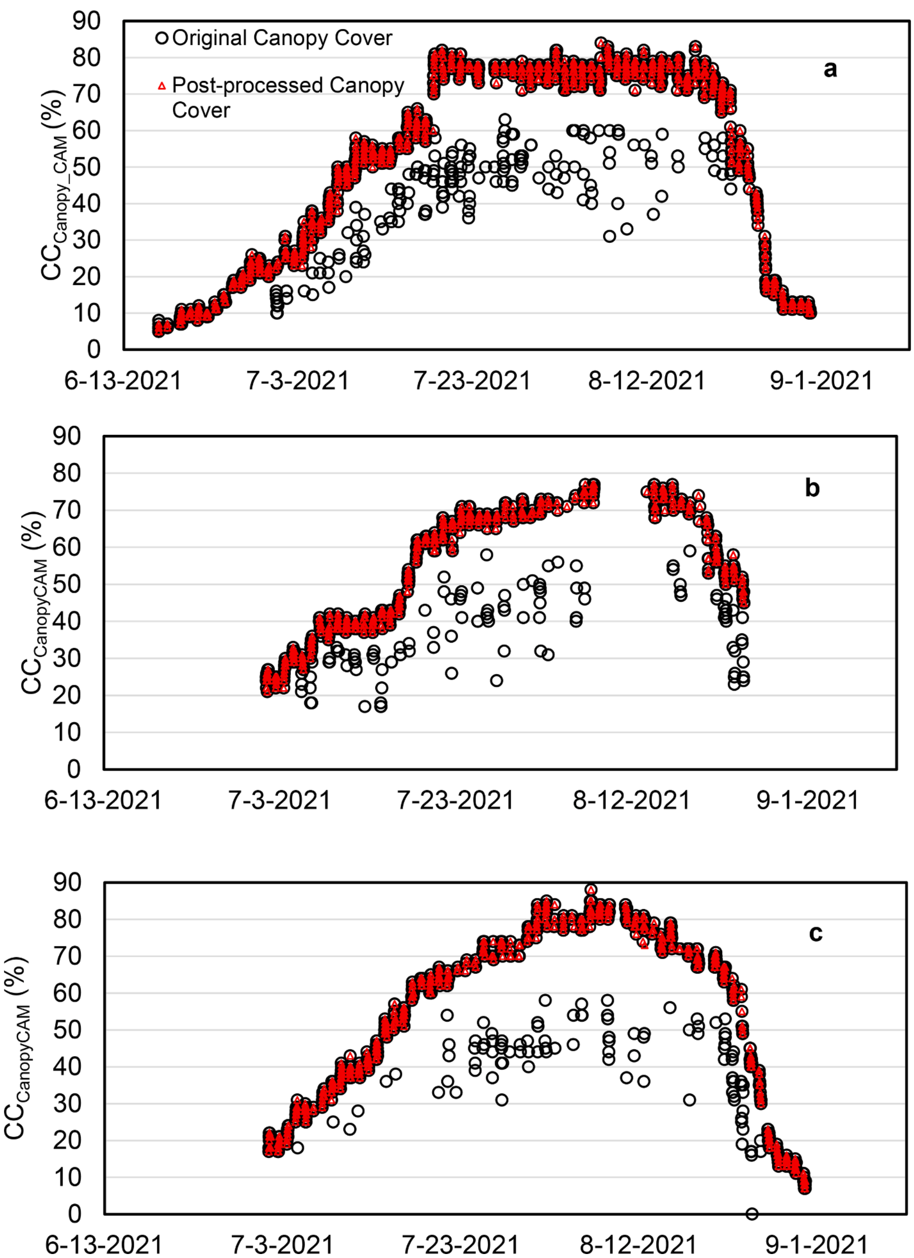

Fig. 7. From top to bottom, original and post-processed canopy cover by CanopyCAM at research plots: R-1 (a), R-2 (b), and R-3 (c).

also be noted that the improved R^2 doesn't mean CC_{max} and t_{max_canopy} were correlated with dry bean yield, at least based on this study's results. Rather, the results here are used to show CC_{max} and t_{max_canopy} can be extracted based on CanopyCAM and demonstrate its potential applications.

3.3. Comparison of different canopy sensing design with CanopyCAM

In recent years, several studies have used image processing and edge-computing concept to determine NDVI, canopy cover, and crop condition (Kim et al., 2019; Chamara et al., 2021; Taylor and Browning, 2022). Kim et al. (2019) developed a Smart Surface Sensing system (4S) that monitor canopy color, vegetation index, leaf area index, and fraction of absorbed photosynthetically active radiation (fPAR) at rice paddy site using Raspberry Pi with a camera, multi-spectral spectrometer, and Wi-Fi for processed data transmission. Compared to Kim et al. (2019), CanopyCAM used LoRaWAN rather than Wi-Fi. The processed results were displayed near real-time at our in-housed website. In addition, CC from CanopyCAM achieved higher performance (RMSE and R^2 were 2.95 % and 0.99 compared to CC derived from LI-COR LAI; R^2 was 0.76 in Kim et al. (2019) compared to Li-COR LAI derived CC).

Chamara et al. (2021) developed a soybean leaf detection algorithm using Deep Convolutional Neural Network (DCNN) and RGB images collected in 30 days using Rapsberry Pi based camera devices. The image taken from the field was reduced from 1920 × 1080 resolution to 512 × 512 resolution to reduce image processing time. They also used LoRaWAN to transmit processed results. The accuracy of green pixel segmentation using DCNN in Chamara et al. (2021) was 94 %. It was not clear how this accuracy value was obtained. While in this study, readings from CanopyCAM were evaluated against a widely used LI-COR plant canopy analyzer with good performance. Compared to Chamara et al. (2021), using our algorithm and configuration of CanopyCAM, the image didn't need to be compressed (image resolution is 2592 × 1944 and can be higher if needed, current processing time 2 ~ 3 seconds). The higher resolution will also imply other uses in the future, such as disease detection, which would require more details from leaves. Furthermore,

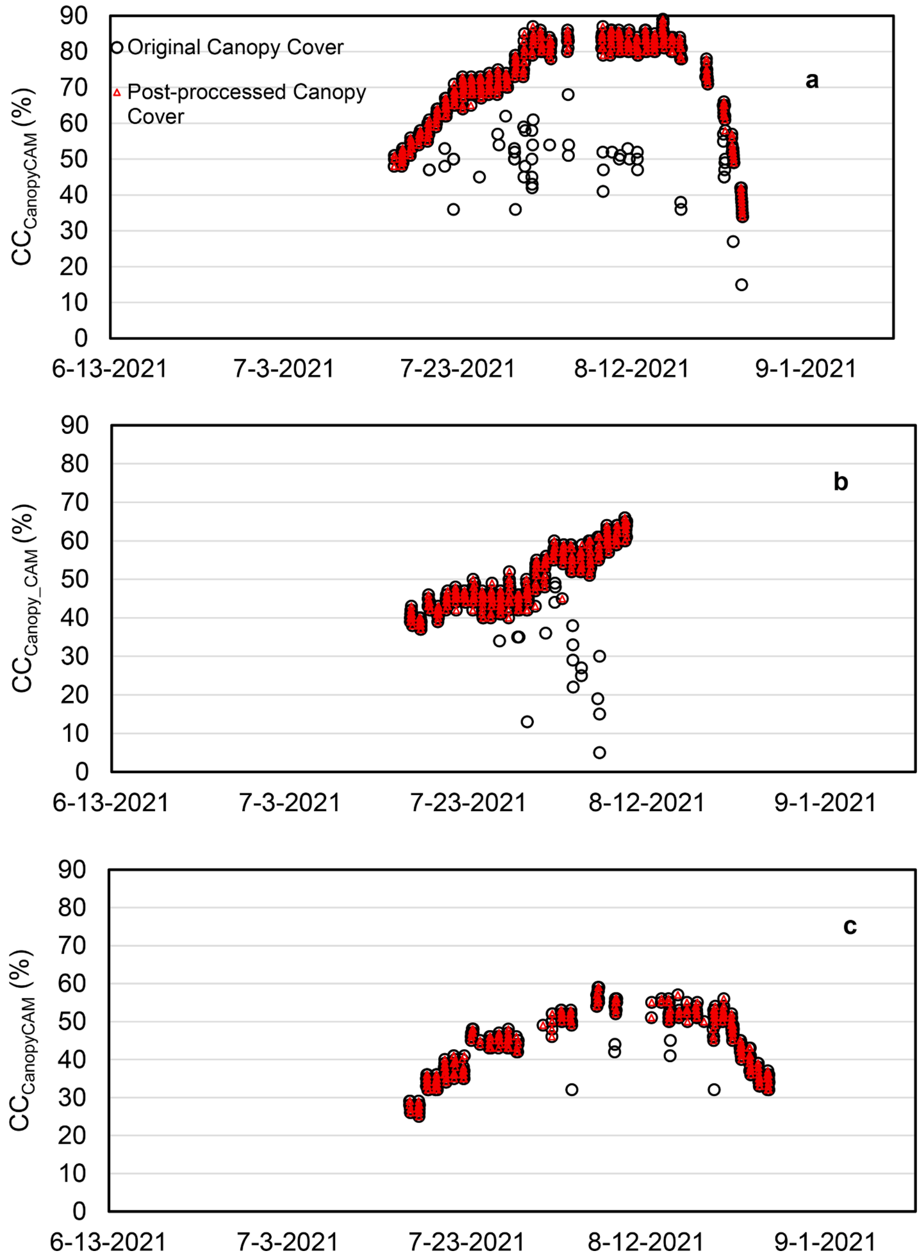

Fig. 8. Original and post-processed canopy cover by CanopyCAM at commercial farms: C-1 (a), C-2 (b), and C-3 (c).

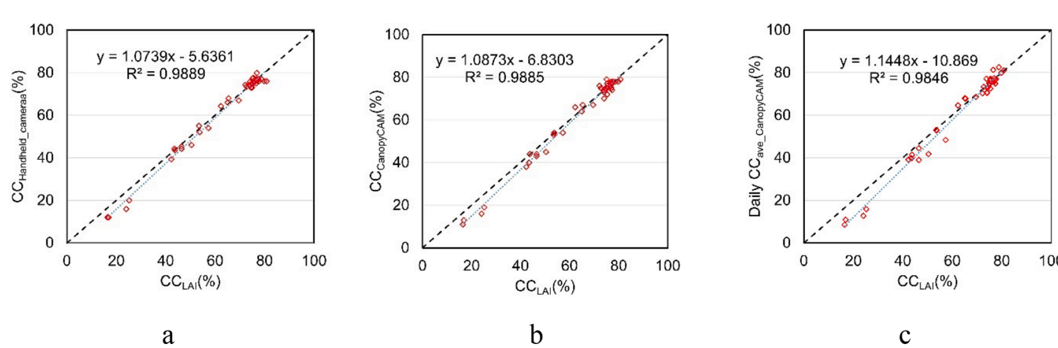

Fig. 9. A. comparison between canopy cover percentage (CC) estimated from LI-COR LAI2000 (cc_{LAI}) and estimated CC with handheld camera using Crop Canopy Image Analyzer ($CC_{Handheld\_camera}$). RMSE = 2.64 %, $p < 0.01$, n = 41; b. comparison between CC_{LAI} and estimated CC using CanopyCAM ($CC_{CanopyCAM}$). RMSE = 2.95 %, $p < 0.01$, n = 41; c. Comparison between CC_{LAI} and estimated daily averaged CC_{Canopy_CAM} ($CC_{ave\_CanopyCAM}$). RMSE = 4.05 %, $p < 0.01$, n = 41. Dotted line is 1:1 line.

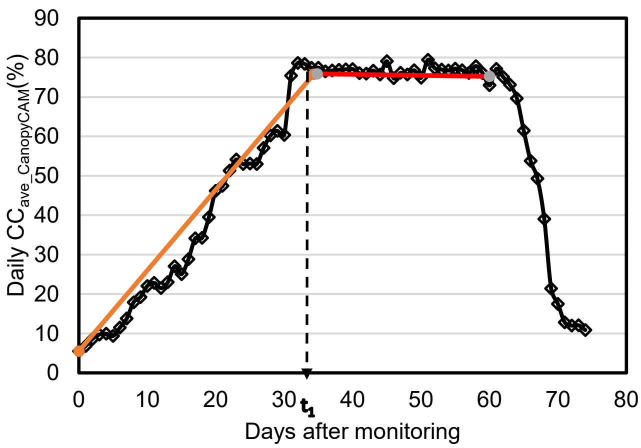

Fig. 10. An example of estimating t_1 using CRG algorithm and constraints at R-1 field. Orange line represented increasing CC of the 1st stage, and red line represented CC of the 2nd stage. (For interpretation of the references to color in this figure legend, the reader is referred to the web version of this article.)

Table 3
Estimated average CC_{max} and t_{max_canopy} of six fields.

Loc.	t_1	t_2	Average CC_{max}, %	t_{max_canopy}, d	Yield, kg ha^{-1}
R-1	48 (7/18)	80 (8/19)	76.6	33	436
R-2	53 (7/23)	80 (8/19)	70.7	28	315
R-3	61 (7/31)	75 (8/14)	78.5	15	329
C-1	63 (7/28)	84 (8/18)	82.2	22	403
C-2	N/A	N/A	N/A	N/A	322
C-3	79 (8/6)	93 (8/20)	53.0	15	268

t_1: days after planting to beginning of maximum canopy cover, and the date shown in parentheses.
t_2: days after planting to end of maximum canopy cover, and the date shown in parentheses.
t_{max_canopy}: duration between t_1 and t_2.
Average CC_{max}: Average maximum canopy cover during t_{max_canopy}.

compared to Chamara et al. (2021), our algorithm was fully developed in house based on different classes of color groups using Mahalanobis distance equation and can be easily customized for different situations. In addition, LoRaWAN-based data transmission in our study was tested in commercial farm settings, where Chamara et al. (2021) tested it in a research farm setting. Lastly, our results can be readily displayed at an in-house developed website and that be viewed by growers and researchers.

Taylor and Browning (2022) developed a PhenoCAM that automatically classify crop phenology, flooded condition and snow-covered fields. Our study focused on continuous monitoring of crop CC rather than crop phenology or field conditions, and thus is different than Taylor and Browning (2022). Also, it is not clear how hardware was set up in Taylor and Browning (2022), or how data was transmitted and displayed.

In summary, compared to previous studies, this research is unique in several aspects: 1) CanopyCAM is a complete solution with hardware and software that can determine crop CC continuously with high accuracy and has been tested at both research and commercial dry bean fields; 2) The algorithm of CanopyCAM was fully developed in house based on different classes of color groups using Mahalanobis distance equation and can be easily adjusted to accommodate different situations; 3) Canopy cover from CanopyCAM has been compared against commercial device (LI-COR plant canopy analyzer) and achieved good performance, and 4) The results can be displayed near real-time at our in-housed programmed website for visualization.

4. Conclusions

This study described the development of software, hardware, and visualization for a IoT edge-computing device – CanopyCAM, that could monitor dry edible beans CC continuously throughout the growing season. The device provided accurate CC readings which could be used by growers and researchers for different purposes. The edge-computing, IoT enabled capability of CanopyCAM, also provided simple, low-cost method to report readings at different user-end interfaces. Key findings were:

1. CanopyCAM was able to provide automatic, real-time, continuous, and accurate CC readings. Among the six deployed CanopyCAM devices during the 2021 growing season, the RMSE of post-processed $CC_{CanopyCAM}$ for each day was 2.2–7.5 % as compared to CC_{LAI} with R^2 of 0.99.

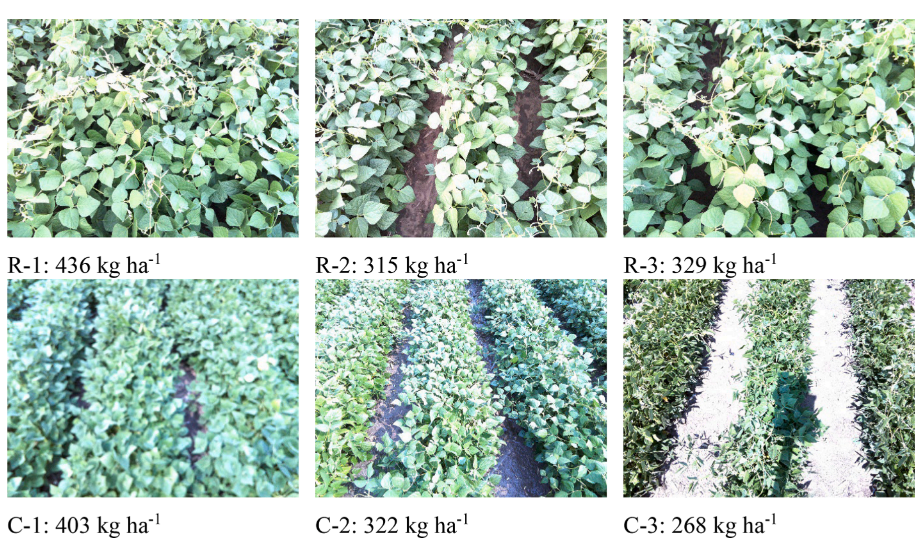

Fig. 11. Maximum canopy cover (CC_{max}) obtained from CanopyCAMs and yield of the six fields.

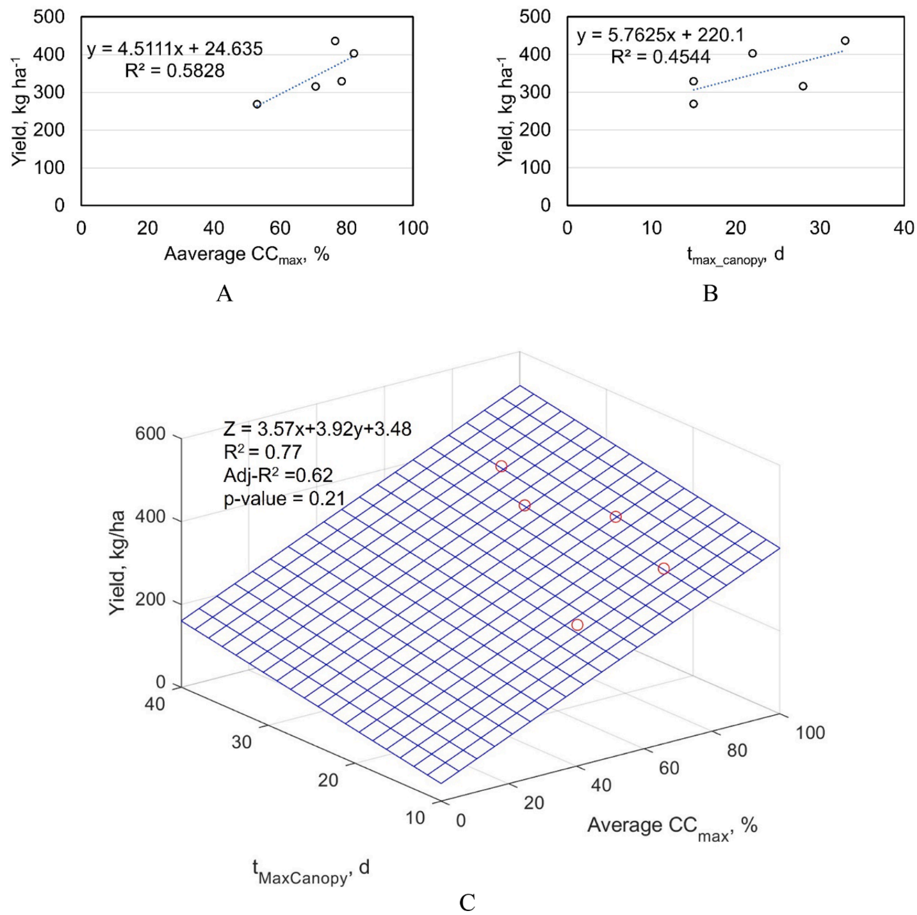

Fig. 12. A. correlation of average cc_{max} with yield ($R^2 = 0.58$, p-value = 0.23); b. Correlation of t_{max_canopy} with yield ($R^2 = 0.45$, p-value = 0.21); c. Correlation of CC_{max} and t_{max_canopy} with yield ($R^2 = 0.77$, Adjusted-$R^2 = 0.62$, p-value = 0.13), x represented Average CC_{max}, y represented t_{max_canopy}, and z represented yield.

2. Based on the continuous monitoring of CC, parameters such as CC_{max} and t_{max_canopy} can be extracted and can be potentially used for different purposes.

Although good performance of CanopyCAM was achieved, there are few limitations. CanopyCAM is still a ground-based, point-sourced measurement device. For large-scale commercial fields, CanopyCAM faces the same challenges as other commercially available ground-based, point-sourced devices such as soil moisture sensors in terms of field heterogeneities from soil types, management, and other environmental variables. Several future work are proposed: 1) redesign the camera casing and add lens hood using 3D printed materials to physically reduce overexposure of images and increase number of usable images; 2) adjust camera settings of CanopyCAM to allow more usable images; 3) broaden the use of CanopyCAM to include disease recognition, weed detection, and crop water use calculation; 4) test CanopyCAM for other crops such as corn and sugar beets; 5) improve spatial resolution of CanopyCAM by mounting CanopyCAM on irrigation system and integrate with GPS.

5. Authorship statements

The authors confirm contribution to the paper as follows: Xin Qiao was responsible for conception and design of the study. Wei-zhen Liang analyzed and interpreted results and drafted the manuscript. Wei-zhen Liang also developed the software and algorithm. Joseph Oboamah designed the hardware. Xin Qiao, Yufeng Ge, Bob Harveson, Daran Rudnick, Jun Wang, and Haishun Yang revised the manuscript critically and contributed intellectual contents. Angie Gradiz was responsible for acquisition of some of data used in this study. All authors reviewed the results and approved the final version of the manuscript.

Declaration of Competing Interest

The authors declare that they have no known competing financial interests or personal relationships that could have appeared to influence the work reported in this paper.

Data availability

Data will be made available on request.

Acknowledgements

We greatly appreciate the financial support from Nebraska Dry Bean Commission on this project. We also would like to acknowledge the funding support from USDA with Award No. 2019-67021-29227. This research project is also supported by the USDA National Institue of Food and Agriculture (Hatch project NEB-21-177, accession number 1015698). We also want to thank the editor and reviewers' constructive comments and suggestions that have significantly improved this manuscript.

References

Adelantado, F., Vilajosana, X., Tuset-Peiro, P., Martinez, B., Melia-Segui, J., Watteyne, T., 2017. Understanding the Limits of LoRaWAN. IEEE Communications Magazine 55 (9), 34–40.

Buchi, L., Wendling, M., Mouly, P., Charles, R., 2018. Comparison of visual assessment and digitao image analysis for canopy cover estimation. Agronomy 110, 1289–1295.
Chamara, A.H.M.N., K. Alkady, H. Jin, F. Bai, A.K. Smal, and Y. Ge. 2021. Deep convolutional neural network based image processing framework for monitoring the growth of soybean crops. ASABE paper #2100259. Annual Meeting, Virtual Meeting. July 12th -16th.
Chen, B., Wan, J., Celesti, A., Li, D., Abbas, H., Zhang, Q., 2018. Edge computing in IoT-based manufacturing. IEEE Communications Magazine 56 (9), 103–109.
Chena, X., Xunb, Y., Li, W., Zhang, J., 2010. Combining discriminant analysis and neural networks for corn variety identification. Computers and Electronics in Agriculture 71, 48–53.
Colaizzi, P.D., Kustas, W.P., Anderson, M.C., Agam, N., Tolk, J.A., Evett, S.R., Howell, T. A., Gowda, P.H., O'Shaughnessy, S.A., 2012. Two-source energy balance model estimates of evapotranspiration using component and composite surface temperatures. *Advances Water Resour*ces 50, 134–151.
Dai, X., Jia, X., Zhang, W., Bai, Y., Zhang, J., Wang, Y., Wang, G., 2009. Plant height-crown radius and canopy coverage-density relationships determine above-ground biomass-density relationship in stressful environments. Biology letters 5 (4), 571–573.
Devroye, L., Gyorfi, L., Lugosi, G., 1996. A probabilistic theory of pattern recognition, 1st Edition. Springer, New York.
Diago, M., Correa, C., Millan, N., Barreiro, P., Valero, C., Tardaguila, J., 2012. Grapevine yield and leaf area estimation using supervised classification methodology on RGB images taken under field conditions. Sensors 12, 16988–17006.
Drewry, D.T., Kumar, P., Long, S., Bernacchi, C., Liang, X.-Z., Sivapalan, M., 2010. Ecohydrological responses of dense canopies to environmental variability: 1. Interplay between vertical structure and photosynthetic pathway. Geophysics Research: Biogeoscience 115 (G4).
García-Martínez, H., Flores-Magdaleno, H., Ascencio-Hernández, R., Khalil-Gardezi, A., Tijerina-Chávez, L., Mancilla-Villa, O.R., Vázquez-Peña, M.A., 2020. Corn Grain Yield Estimation from Vegetation Indices, Canopy Cover, Plant Density, and a Neural Network Using Multispectral and RGB Images Acquired with Unmanned Aerial Vehicles. Agriculture 20 (7), 277.
Harveson, R.M., Steadman, J.R., and Schwarz, H.F. 2013. White mold of dry beans. Nebguide G1786. University of Nebraska-Lincoln.
Hitimana, E., Gwun, O., 2014. Automatic estimation of live coffee leaf infection based on image processing techniques. In: Second International Conference on Signal, Image, Processing and Pattern Recognition, pp. 255–266.
Hoffman, H., Nieto, H., Jensen, R., Guzinski, R., Zarco-Tejada, P., Friborg, T., 2016. Estimating evaporation with thermal UAV data and two-source energy balance models. Hydrology Earth System Science 20, 697–713.
Kim, J.Y., Ryu, C.J., Hwang, Y., 2019. Continuous observation of vegetation canopy dynamics using an integrated low-cost, near-surface remote sensing system. Agricultural and Forest Meteorology 264, 164–177.
Liang, W.-Z., Kirk, K.R., Greene, J.K., 2018. Estimation of soybean leaf area, edge, and defoliation using image analysis. Computers and Electronics in Agriculture 150, 41–51.
Liang, W.-Z., Possignolo, I., Qiao, X., DeJonge, K., Irmak, S., Heeren, D., Rudnick, D., 2021. Utilizing digital image processing and two-source energy balance model for the estimation of evapotranspiration of dry edible beans in western Nebraska. Irrigation Science 39 (5), 617–631.
Ma, B.L., Dwyer, L.M., Costa, C., Cober, E.R., Morrison, M.J., 2001. Early prediction of soybean yield from canopy reflectance measurements. Agronomy 93 (6), 1227–1234.
Malone, S., Herbert, D.M., Holshouser, D.L., 2002. Evaluation of the LAI-2000 plant canopy analyzer to estimate leaf area in manually defoliated soybean. Journal of Agronomy 94, 1012–1019.
Masood, R., Khan, S.A., Khan, M.N.A., 2016. Plants disease segmentation using image processing. *I.J.* Modern Education and Computer Science 1, 24–32.
NDBC. Nebraska Dry Bean Commission. 2019. http://nebraskadrybean.nebraska.gov.
Norman, J.M., Kustas, W.P., Humes, K.S., 1995. A two-source approach for estimating soil and vegetation energy fluxes from observations of directional radiometric surface temperature. Agriculture Forestry Meteorology 77, 263–293.
NDSU. North Dakota State University dry bean production guide. 2019. https://www.ag.ndsu.edu/publications/crops/dry-bean-production-guide.
O'Neal, M.E., Landis, D.A., Issacs, R., 2002. An inexpensive, accurate method for measuring leaf area and defoliation through digital image analysis. Journal of Economic Entomology 95 (6), 1190–1194.
Patrignani, A., Ochsner, T.E., 2015. Canopeo: a powerful new tool for measuring fractional green canopy cover. Agronomy 107, 2312–2320.
Qiao, X., Farahani, H.J., Khalilian, A., Barnes, E.M., 2016. Cotton water productivity and growth parameters in the humid southeast: experimentation and modeling. Transactions of the ASABE 59 (3), 949–962.
Reed, V., Arnall, D.B., Finch, B., Souza, J.L.B., 2021. Predicting winter wheat grain yield using fractional green canopy cover (FGCC). International Journal of Agronomy 2021, 1443191.
Schmitz, P.K., Kandel, H.J., 2021. Using Canopy Measurements to Predict Soybean Seed Yield. Remote Sensing 13 (16), 3260.
Taylor, S.D., Browning, D.M., 2022. Classification of daily crop phenology in PhenoCams using deep learning and hidden Markov models. Remote Sensing 14, 286.
Tenreiro, T.R., García-Vila, M., Gómez, J.A., Jiménez-Berni, J.A., Fereres, E., 2021. Using NDVI for the assessment of canopy cover in agricultural crops within modelling research. Computers and Electronics in Agriculture 182, 106038.
Westgate, M.E., Forcella, F., Reicosky, D.C., Somesen, J., 1997. Rapid canopy closure for maize production in the northern US corn belt: Radiation-use efficiency and grain yield. Field Crops Research 49 (2), 249–258.
Yang, Y., Qiu, J., Zhang, R., Huang, S., Chen, S., Wang, H., Luo, J., Fan, Y., 2018. Intercomparison of three two-source energy balance models for partitioning evaporation and transpiration in semiarid climates. Remote Sensing 10, 1149.